Observations and Simulations of Transverse Density Waves in a Collimated Space-Charge Dominated Electron Beam

S. Bernal, R. A. Kishek, and M. Reiser
Institute for Plasma Research, University of Maryland, College Park, Maryland 20742

I. Haber
Naval Research Laboratory, Washington, D.C. 20375
(Received 4 February 1999)

Experiments and particle-in-cell simulations demonstrate the appearance of wavelike transverse density variations in a space-charge dominated electron beam. Simulations show how an aperture located near the source gives rise to a nonequilibrium phase-space distribution with strong force imbalance confined to a sheath near the beam edge. Tracking of particles in this sheath, starting near the aperture's edge, reproduces well the onset of the perturbation. The subsequent evolution of the perturbation over about one meter suggests the appearance of a transverse wave. For the parameters investigated, simulations further indicate that the perturbation damps out over a few plasma periods without causing any rms emittance growth. [S0031-9007(99)09152-8]

PACS numbers: 29.27.Bd, 41.85.Ja

The detailed physics of space-charge dominated beam transport is of interest to basic research as well as to many applications such as heavy ion fusion, spallation neutron sources, and others where intense beams of high quality are required. Many studies [1,2] have dealt with equilibrium and stability properties of space-charge dominated beams. A rarely discussed aspect concerns the evolution of beams from the source to equilibrium, if any, including the role of source errors or aberrations, apertures and other factors that affect the initial particle distribution in phase space. The initial density profile of a beam has long been recognized as an important factor in determining its evolution (i.e., rms emittance growth, instabilities, etc.) [3]. A less appreciated influence on the dynamics is the initial temperature profile of the beam. A simple and tractable equilibrium distribution that is widely used to model real intense beams is the Kapchinskij-Vladimirskij (K-V) distribution [4], which has uniform density in both space and velocity. Using a K-V distribution, Gluckstern [2,5] has derived transverse kinetic oscillation modes that involve an exchange between the thermal and field energies. While these modes are harmless in the case of the uniformly focused beam treated by Gluckstern, they can cause instabilities in a periodic transport channel [1]. Using a warm-fluid model, Lund and Davidson [6] have rederived the Gluckstern modes and extended them to non-K-V equilibrium distributions. Further, recent computer simulations by Lund *et al.* [7], relating to experiments at Lawrence Berkeley National Laboratory, exhibit density oscillations similar to Gluckstern modes, in a beam whose initial temperature or density profiles are perturbed. Despite the important insights provided by these studies, no clear connection has been established in either experiments or simulations between the physical cause(s) of the initial beam perturbation, the resulting phase-space distribution, and the long term evolution of this distribution.

This Letter presents concrete experimental evidence, augmented by self-consistent particle-in-cell (PIC) computer simulations, for the occurrence of collective transverse density oscillations in an electron beam. The beam is perturbed by an aperture near the source, giving rise to an initial distribution that is far from equilibrium around the beam's edge. The simulations demonstrate the importance of the combined role of the initial temperature and density profiles; when extended to several periods of the focusing channel, the simulations illustrate the evolution of the beam particle distribution towards equilibrium. The model is further probed by tracking of test particles starting at the aperture and moving near the beam's edge. In so doing, a particle-flow component to the initial perturbation is revealed, which eventually may give way to a transverse density wave.

A number of different lattices were employed to experimentally study the onset and evolution of the beam perturbation. Figure 1 shows the schematics of a transport experiment with three solenoids. The electron gun, a Pierce-type source, produces 4 keV, 175 mA pulses (5 μs) at a rate of 60 Hz. An aperture, 6.4 mm in diameter, is placed 12.4 cm from the cathode; the aperture size is

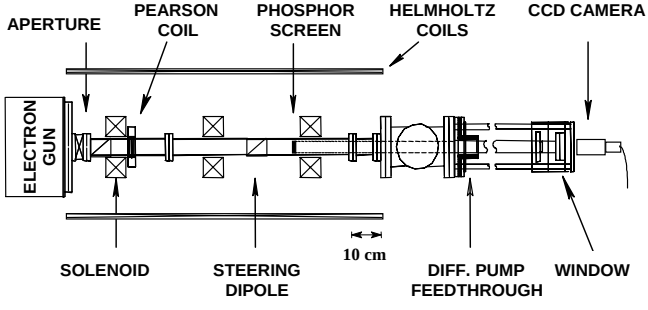

FIG. 1. Three-solenoid experiment setup.

 0031-9007/99/82(20)/4002(4)$15.00

roughly $1/3$ the full beam size at that plane and results in an almost uniform, 17 mA beam entering the transport pipe. The transport experiments use short solenoids, of the type employed extensively at Maryland, and printed-circuit (PC) air-core magnetic quadrupoles, introduced recently for the University of Maryland electron ring [8] which is currently under construction. The strengths of focusing elements are chosen for rms envelope matching into a periodic lattice with a zero-current phase advance of $\sigma_0 = 85°$. This corresponds to an average beam radius close to 0.75 cm. The ratio of phase advances with and without space charge, σ/σ_0, is typically 0.3, in the regime of strongly space-charge dominated beam transport.

The beam diagnostics is a 2.54 cm (diameter) phosphor screen that can be moved from the aperture out to a distance of nearly 1 m. The beam pictures are captured with a charge-coupled device (CCD) camera and then digitized and displayed using associated hardware and software. For the first experiments, we used a single solenoid located at 12.5 cm from the aperture; to extend the transport distance, two solenoids were added and experiments performed with different overall focusing strengths. Finally, an all-quadrupole lattice was employed, as well as a solenoid-five PC quad combination. In all cases, a bright ring appears along the beam's edge at a distance downstream from the aperture that depends on the strength of the first element (a solenoid or a quadrupole doublet).

For illustration, the fluorescent screen pictures from typical experiments with three solenoids and six PC quadrupoles are summarized in Figs. 2(a),2(b), top parts. The solenoids are located at 12.5, 36.5, and 66.5 cm from the aperture and have effective lengths equal to 4.50, 3.99, and 3.87 cm. Their peak on-axis fields are 62.8, 45.9, and 56.6 G. The first picture on the left-hand side in Fig. 2(a), top, is taken between the first two solenoids, and the second one is taken near the plane of the second solenoid. At these two planes, the beam is fairly uniform; the ring is first seen at about 45 cm from the aperture, after roughly 10 cm from the first beam waist. Further downstream, the ring moves inwards relative to the beam's edge, and a second ring emerges around 86 cm from the aperture.

Similar rings are observed in alternating-gradient focusing systems. In the all-quadrupole experiment, the lenses have the same effective length (3.35 cm) and are located at 4.7, 10.5, 20.8, 33.0, 47.3, and 63.3 cm from the aperture. The magnitudes of the peak field gradients are 9.9, 11.6, 7.7, 5.4, 5.4, and 5.8 G/cm. As in the three-solenoid case, the ring appears at about 45 cm from the aperture, near the plane of quadrupoles 5.

To aid in understanding the experiment, we have conducted 2D and 3D PIC simulations using the code WARP [9]. Details of the numerics and modeling of focusing elements are described thoroughly elsewhere in connection with simulations of the Maryland electron ring [10]

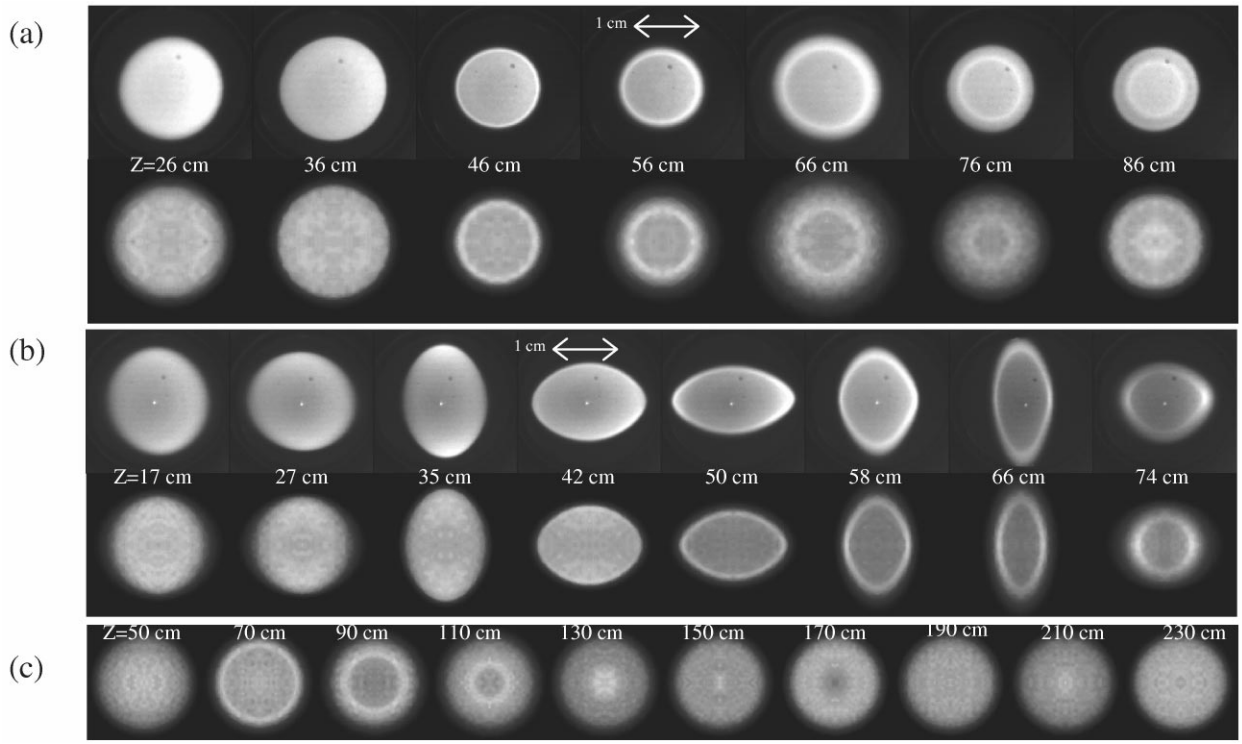

FIG. 2. Summary of experiments and simulations: (a) three-solenoid experiment—phosphor screen pictures (top), and PIC simulations (bottom); (b) six PC-quadrupole experiment—phosphor screen pictures (top), and PIC simulations (bottom); and (c) simulation of uniform focusing case, where the (matched) beam size is constant (0.8 cm in radius). In all cases, $z = 0$ is the location of the aperture plane. In (a) and (b), the scales of experimental and simulation pictures are slightly different.

and prototype injector experiments [11]. To compare the beam density distributions with the experiments, the particles are loaded on a 256 × 256 (typically) mesh across the 1.5″ diameter beam pipe. The particle density distribution on that mesh is then extracted and displayed so that it resembles phosphor screen pictures. Typically, 100 000–200 000 particles are used to obtain reasonably smooth pictures. As is evident from Figs. 2(a),2(b), (bottom), the rings are also observed in the simulations, and agreement between the simulation and the experiment is good, although a difference in the phase of the perturbation is seen, more noticeably in the three-solenoid case.

The simulations especially address the role of initial conditions. In the simplest approximation, the beam emerging through the aperture is modeled with a semi-Gaussian (S-G) distribution, i.e., one that is uniform in space, but has a Gaussian velocity distribution corresponding to a radially uniform temperature. The phase of the perturbation, however, is sensitive to the temperature profile, so starting the simulations at the beam waist upstream from the aperture [Fig. 3(a)], and fully modeling the latter, results in better agreement with experiment. In this case, we observe that the truncated distribution has a nonuniform temperature profile resulting from aperturing of an expanding beam [Figs. 3(b),3(c)]. Alternatively, a S-G distribution with a parabolic temperature profile right after the aperture produces similar results.

We gain additional insight for understanding the density perturbation when we replace the truncated distribution in the simulation with an rms equivalent equilibrium distribution, such as a K-V. In that case, no rings appear whatsoever, and the beam distribution remains K-V for the rest of the channel. This leads us to believe that the wavelike perturbation is the result of a force imbalance or lack of equilibrium in a sheath at the beam edge, right after the aperture. As seen in Fig. 3(c), the phase space is trapezoidal and tilted, with anomalous particle populations with relatively large velocities near the beam edge. In addition, the distribution lacks the spatial tails of an equilibrium thermal distribution (Maxwell-Boltzman), which are of the order of a Debye length [1]. In our case, the Debye length is 0.74 mm, which is non-negligible when compared to the beam radius near (and downstream of) the aperture, so the fraction of "missing" particles in a sheath one Debye length is significant. In summary, the truncated distribution is not only a nonequilibrium distribution, but also one where the departure from equilibrium is confined to the beam edge. As a consequence, the beam-edge particles experience space-charge forces that are very different from those affecting the particles in the bulk of the beam. The combined effects of nonlinear space-charge forces near the beam edge, and linear external focusing produce the beam evolution illustrated in Figs. 3(d)–3(f) for the simulation of the six-quadrupole experiment.

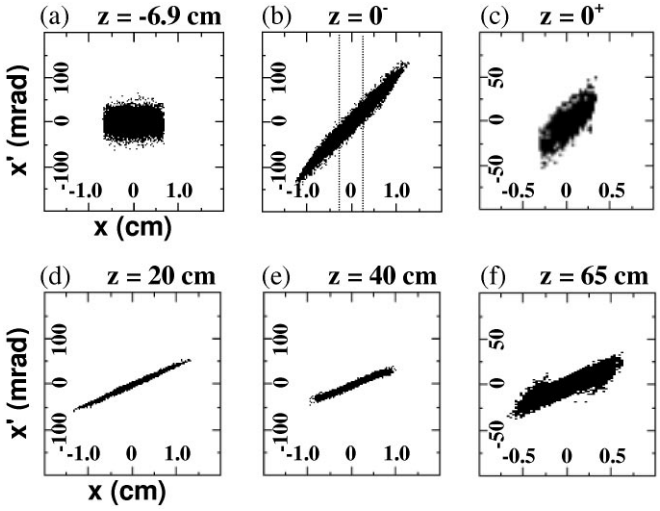

FIG. 3. Horizontal projection of phase space at (a) the beam waist, 6.9 cm upstream of the aperture, (b) the upstream plane of the aperture—the dashed lines indicate the 0.32 cm (radius) aperture, (c) the downstream plane of the aperture, and (d)–(f), evolution in the all-quadrupole lattice—note the blown-up scales in (c) and (f).

If the particles at the tips of the trapezoidal distribution of Fig. 3(c) are tracked, and their radial locations compared to the locations of the rings in pictures from experiment or simulations, a correlation is established in the initial stage. In other words, an electron flow component is seen that explains the appearance of the first ring; the second ring [see Fig. 2(a)], however, is most likely the result of a charge density perturbation induced by the initial flow. The use of single-particle equations in a K-V beam model, i.e., assuming the space-charge forces arise from a uniform density beam with a sharp edge, also reproduces correctly the onset of the perturbations in all experiments. In the model, the particles leave the beam near the edge of the aperture and are focused back into the beam, the self-potential for the bulk of the beam changing from logarithmic, outside, to harmonic, inside. Figure 4 shows the results of these calculations for the three-solenoid experiment of Fig. 2(a).

Finally, to examine the long term evolution of the beam, simulations were done in a uniform focusing channel over a distance of 20 m. The simulations are a "smooth approximation" version of the three-solenoid case; i.e., the beam has the same generalized perveance, and it is matched so its radius is constant, comparable to the average beam size in the experiments. As seen in Fig. 2(c), the perturbation appears at a distance of about 70 cm from the aperture, and the oscillations persist for a few plasma periods ($\lambda_p \sim 1$ m in this case) and eventually diminish in amplitude as the beam evolves into equilibrium. Over the extent of the simulations, we observed no rms emittance growth associated with the perturbation, unlike other relaxation mechanisms [1]. Instead, the rms emittance oscillates about its initial value, then levels off to a slightly smaller value as the perturbation damps out.

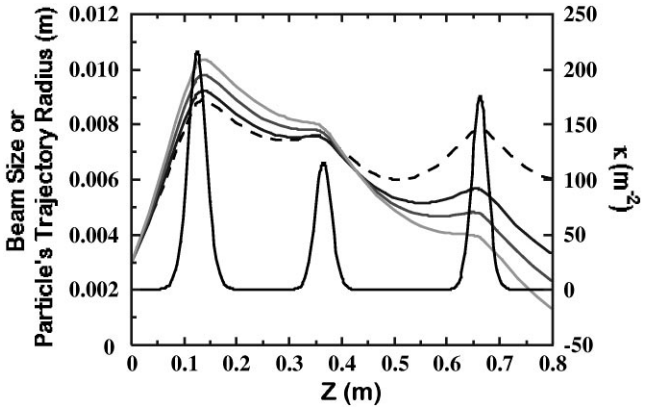

FIG. 4. Trajectory calculations of beam-edge test particles in the three-solenoid experiment of Fig. 2(a). For purposes of illustration, the initial slopes of particle orbits are 40, 45, and 50 mrad, but the actual range is smaller [see Fig. 3(c)], centered around 40 mrad. The dashed curve represents the beam envelope. The focusing function $\kappa(z)$ is proportional to the square of the solenoid magnetic field.

This seemingly counterintuitive result, where an irreversible change in the beam does not ensue a growth in rms emittance, is consistent with previous simulations with S-G distributions over a few plasma periods [1,3]. Apparently, the excess thermal energy of the S-G distribution is converted to field energy in the relaxation process. In a more general context, the rms emittance has been shown not to necessarily increase in the presence of nonlinear forces [12].

To summarize, the experiments and simulations presented clearly demonstrate the existence of a perturbation mechanism that may lead to oscillation modes similar to those derived for ideal K-V beams. The perturbation is the result of a strong beam-edge imbalance produced by an aperture in an expanding beam. Furthermore, the initial nonequilibrium beam distribution can be modeled approximately with a S-G distribution with a nonuniform temperature profile. The corresponding velocity distribution is so distorted that the edge particles initially evolve independently of the bulk of the beam, and, with the use of external focusing, are brought back near to and inside of the beam edge. Under these conditions, simulations show that a collective mechanism for relaxation to equilibrium can exist without an accompanying growth in rms emittance.

Since beam collimation is used in many systems, the phenomenon described here may be fairly universal and worth additional studies. First, a wider range of parameters and conditions (generalized perveance, rms emittance, aperture size and location, external focusing, etc.) in both experiment and simulations has to be explored to answer important questions about scaling, stability of the oscillations, and rms emittance growth. Second, the suggestion that the collective phenomena involve two components must be further studied to understand the extent of the particle-flow component and how it gives rise to a transverse wave. Finally, an interesting thought is the possibility of placing apertures of different sizes at special locations to tailor initial beam distributions with special phase-space properties. These specially prepared beams could in turn be used to study a multitude of collective phenomena.

We acknowledge helpful assistance in the experiments and processing of photos from M. Pruessner and K. Danylevich. We also thank A. Friedman, D. Grote, and S. Lund for support with the WARP code, and D. Kehne, M. Venturini, and J. G. Wang for useful discussions. The work is supported by the U.S. Department of Energy.

[1] M. Reiser, *Theory and Design of Charged-Particle Beams* (Wiley & Sons, New York, 1994), Chap. 6, and references therein.
[2] R. C. Davidson, *Physics of Nonneutral Plasmas* (Addison-Wesley, Reading, MA, 1990).
[3] T. P. Wangler *et al.*, IEEE Trans. Nucl. Sci. **32**, 2196 (1985).
[4] I. M. Kapchinskij and V. V. Vladimirskij, in *Proceedings of the International Conference on High Energy Accelerators, Geneva, 1959* (CERN, Geneva, 1959), p. 274.
[5] R. L. Gluckstern, in *Proceedings of the Linac Conference* (Fermilab, Batavia, IL, 1970), p. 811.
[6] Steven M. Lund and Ronald C. Davidson, Phys. Plasmas **5**, 3028 (1998).
[7] S. M. Lund *et al.*, Nucl. Instrum. Methods Phys. Res., Sect. A **415**, 345 (1998).
[8] M. Reiser *et al.*, Fusion Eng. Des. **32–33**, 293 (1996).
[9] A. Friedman, D. P. Grote, and I. Haber, Phys. Fluids B **4**, 2203 (1992).
[10] R. A. Kishek, S. Bernal, M. Venturini, M. Reiser, and I. Haber, in Proceedings of the International Computational Accelerator Physics Conference, ICAPS, 1998 (to be published).
[11] S. Bernal *et al.*, Phys. Rev. ST Accel. Beams **1**, 044202 (1998).
[12] J. D. Lawson, *The Physics of Charged-Particle Beams* (Clarendon Press, Oxford, 1988), 2nd ed., App. 5; Patrick G. O'Shea, Phys. Rev. E **57**, 1081 (1998).